Available online at www.sciencedirect.com
ScienceDirect
Bioorganic & Medicinal Chemistry 15 (2007) 3539–3547
Bioorganic & Medicinal Chemistry

Conformational analysis of endomorphin-2 analogs with phenylalanine mimics by NMR and molecular modeling

Xuan Shao,[a] Yanfeng Gao,[a] Chuanjun Zhu,[b] Xuehui Liu,[b] Jinlong Yao,[a] Yuxin Cui[b,*] and Rui Wang[a,c,*]

[a]*State Key Laboratory of Applied Organic Chemistry, Institute of Biochemistry and Molecular Biology, School of Life Science, Lanzhou University, Lanzhou 730000, People's Republic of China*
[b]*State Key Laboratory of Natural and Biomimetic Drugs, School of Pharmaceutical Sciences, Medical and Health Analysis Center, Peking University, Beijing 100083, People's Republic of China*
[c]*State Key Laboratory for Oxo Synthesis and Selective Oxidation, Lanzhou Institute of Chemical Physics, Chinese Academy of Science, Lanzhou 730000, People's Republic of China*

Received 20 December 2006; revised 22 February 2007; accepted 23 February 2007
Available online 3 March 2007

Abstract—We investigated a series of conformations of endomorphin-2 (EM-2) analogs substituted by phenylglycine (Phg) and homophenylalanine (Hfe) in the position 3 or 4 by two-dimensional ^{1}H NMR spectroscopy and molecular modeling. Evaluating the aromatic interactions and the dihedral angles in these phenylalanine mimics, we have observed that the conformations in *trans* isomer have varied from extended to folded as bioactivity decreases. It is suggested that the flexibility of aromatic side chain affects the backbone of EM-2 to adopt folded structures, which may block the ligands in binding to μ-opioid receptor.

1. Introduction

One of the less well-understood but significant weak interactions in nature is the aromatic interaction, which is a contributor to stabilize the conformation in peptide and protein.[1–3] This noncovalent interaction through the close packing of aromatic rings is important in the stabilization of some turn structures instead of intramolecular H-bonds.[4–6] And in the case of ligand–receptor binding, the aromatic groups have relevant functions as the directional forces that insert into the hydrophobic core of receptors.[7–9] Endomorphin-1 (EM-1, Tyr^1-Pro^2-Trp^3-Phe^4-NH_2) and endomorphin-2 (EM-2, Tyr^1-Pro^2-Phe^3-Phe^4-NH_2) are endogenous opioid peptides isolated from the bovine brain and exhibit the highest selectivity and affinity for the μ-opioid receptor among the endogenous peptides elucidated so far.[10] But how they display their functions, by what preferred types of conformations, in binding to μ-opioid receptor has not been clarified.[11] Nevertheless, with the abundance of aromatic amino acids and flexibility, they are the ideal models to reveal the aromatic interactions on predicting the conformations as ligands.[12]

The conformation of EM-1 has been discussed in more detail than that of EM-2. The *cis*-EM-1 adopted a compact sandwich structure in DMSO, in which the aromatic rings of Tyr^1 and Trp^3 are packed against Pro^2,[13] whereas in aqueous solution and different micelles, Tyr^1 and Phe^4 play a role in the stabilization of the structure of *trans*-EM-1.[14] As for the conformational study of EM-2, only a few results about the analogs with modified C-terminus have been proposed by several groups.[15–17] In addition, some theoretical molecular dynamics simulations about the conformations of EM-1 and EM-2 have been investigated in detail.[12,18–21] The subsequent considerable efforts on bioactive conformation and structural determinants of the EMs have also been probed by testing structure–activity relationship about different types of analogs.[22–25] On the basis of a similarity between the three-dimensional structure and the receptor selectivity profile of EMs, some studies on analogs containing β-turn mimetic,[26] D-configuration[17,27] or pseudoprolines[28] reveal many important

Keywords: Endomorphin-2; Conformation; NMR; Molecular modeling.
* Corresponding authors. Tel.: +86 10 82802377; fax: +86 10 82802377 (Y.C.), tel.: +86 931 8912567; fax: +86 931 8911255 (R.W.); e-mail addresses: yxcui@bjmu.edu.cn; wangrui@lzu.edu.cn

0968-0896/$ - see front matter © 2007 Elsevier Ltd. All rights reserved.
doi:10.1016/j.bmc.2007.02.050

structural information. According to the 'message-address concept',[29] that defines the tripeptide fragment Tyr[1]-Pro[2]-Phe[3] as the message and the C-terminal Phe[4]-NH_2 as address in EM-2, Phe in position 3 and 4 have different functions. Therefore, the aromatic amino acids including phenolic functional groups of Tyr[1] together with the aromatic side chains of Trp[3] or Phe[3] and Phe[4] are essential for opioid receptor recognition.[30]

In our previous report, we have obtained analogs of EM-2 substituted by homophenylalanine (Hfe) and phenylglycine (Phg) (L or D) in position 3 or 4 (Fig. 1), respectively, which could not only keep the aromatic property of phenylalanine but also resist the enzymatic degradation.[31] The analog containing Hfe has higher potency than Phg in position 3, while similar analogs in position 4 show opposite activity. The potency order with the K_i values against the binding of [^{3}H]-DAMGO to μ-opioid receptor is analog 5 > 2 > 3 > 7 > 4 > 6. In the present study, we further investigated these analogs by 1D and 2D ^{1}H NMR spectroscopy to reveal the structural variation of the different surrogates in different positions. The molecular modeling, including energy minimization, distance geometry search, and molecular dynamics, was carried out. The conformations of EM-2 and its analogs were generated by NOE restraints. And several steric structural analyses of aromatic interactions and dihedral angles about the flexibility of side chain occurring in different positions were discussed.

2. Results and discussion

2.1. NMR resonance assignments

Since the EM-2 analogs containing unnatural amino acids have very poor solubility in water, we performed NMR investigations of these analogs using standard one- and two-dimensional NMR spectroscopy in DMSO-d_6 at 298 K. The ^{1}H NMR spectrums of two typical highly potent analogs, analogs 5 ([Phg][4]EM-2)

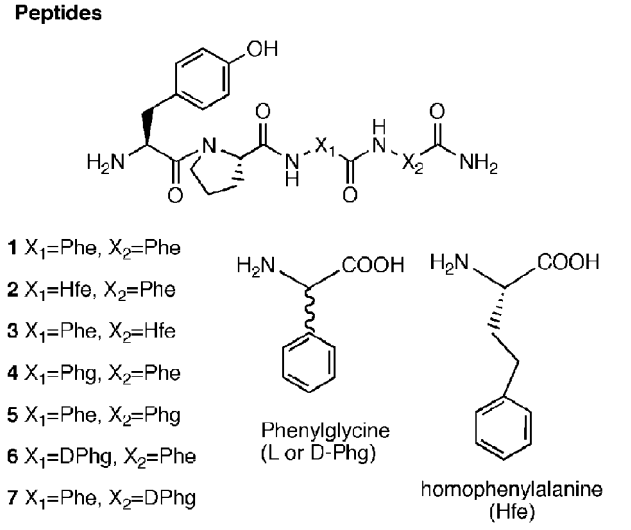

Figure 1. Schematic diagram of EM-2 and its analogs discussed in the present study.

and 2 ([Hfe][3]EM-2), with similar potent antinociceptive activity as that of EM-2, exhibited two populations of conformers distinctly in the peaks of amide and aromatic protons in DMSO-d_6, respectively (Fig. 2). The *cis*/*trans* isomers around the Tyr[1]-Pro[2] amide ω bond were based on the characteristic sequential NOEs observed between the Tyr[1] CαH and Pro[2] CαH protons. The *cis*/*trans* ratios of EM-2 and its analogs compared by the intensities of same protons in *trans* and *cis* isomers are given in Table 1.

It was reported that EM-2 is in equilibrium between folded and open conformers with *cis*/*trans* population ratios of 1:2 in DMSO-d_6.[15] In contrast, we observed that the *trans* isomers in analogs of EM-2 substituted in position 3 were more those in position 4, indicating that *cis* isomers are instable when the distance of aromatic side chain in position 3 is prolonged or shortened. Especially for analog 6 ([DPhg][3]EM-2), which totally lost potency in our previous bioactivity assay,[31] its *trans* isomer was predominant in this solution with *cis*/*trans* ratio 1:5. It further suggests that the flexibility of the aromatic ring and chirality of amino acid in position 3 may be a crucial structural prerequisite in balancing the *cis*/*trans* ratio in solution because of its close relationship with the spacer Pro[2].

The assignments of proton peak for EM-2 and its analogs were performed by combination of connectivity information via scalar coupling in TOCSY experiments and the sequential NOE network cross peaks along the peptide backbone protons. The aromatic ring protons were not resolvable because of chemical shift overlap in this region. Following the protocol of structural determination in solution, the chemical shifts of two main conformations of analogs 5 and 2 are summarized in Table 2, which represent two different kinds of phenylalanine mimics. Variable temperature NMR experiments show no evidence for internal hydrogen bonding for either the *cis* or *trans* isomer.

NOE cross-peaks determined from ROESY spectra using correlation between signal strength and interatomic distances were applied in restraint structural calculation. The amide and aromatic proton districts of ROESY spectrums of analogs 5 and 2 are shown in Figure 3, illustrating the correlation cross peaks of sequential Cα_iH and N_{i+1}H in *trans* and *cis* isomers along with adjacent amino acids. Based on the scalar defining the distance between two protons bonded in the same carbon atom as 1.70 Å, the NOE cross peaks for the *trans* and *cis* isomers were classified as weak (1.6–5.0 Å), medium (1.6–3.6 Å), and strong (1.6–2.9 Å). All NOE cross peaks of EM-2 and its analogs were transferred for restraints data except the *cis*-[DPhg][3]EM-2, which is lacking scalar NOE cross peak of proton pairs due to high degree of overlap and existing low *cis* population in DMSO-d_6. We have displayed the NOE cross peaks and intensities of analogs 5 and 2 in Table 3 omitting the correlation protons in the same carbon. Only a few nonsequential ROESY cross peaks were observed for the investigated peptides, which is an indication of the existence of extended conformations in DMSO solution. In addition, the medium or weak interactions between

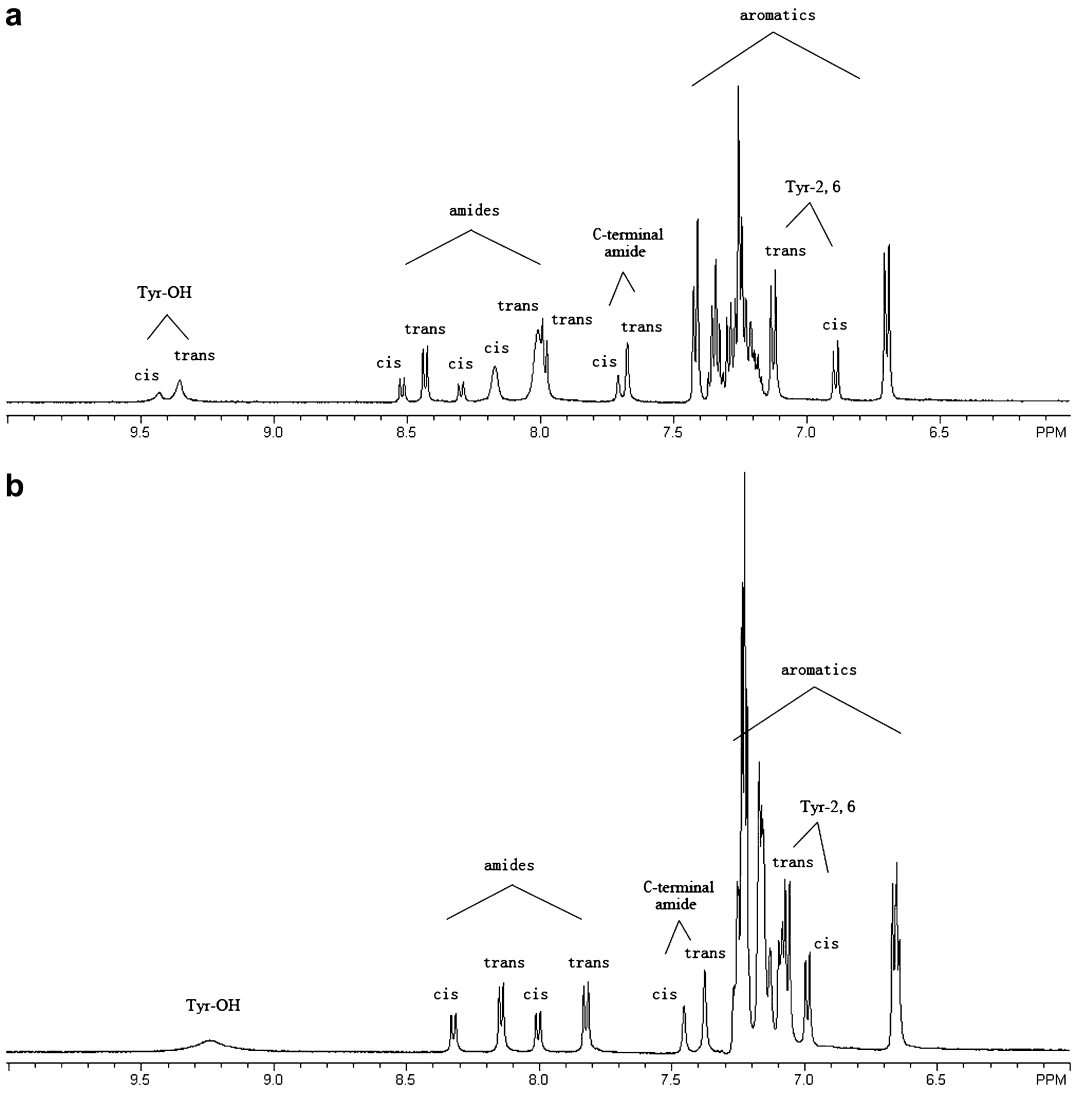

Figure 2. ^{1}H NMR of *cis*/*trans* population observed for the amide and aromatic protons (a) [Phg]^{4}EM-2 and (b) [Hfe]^{3}EM-2 in DMSO-d_6 at 298 K.

Table 1. The *cis*/*trans* ratios[a] of EM-2 and its analogs in DMSO-d_6 at 298 K

No.	Peptides	*cis*/*trans*
1	EM-2	1:2
2	[Hfe]^{3}EM-2	2:5
3	[Hfe]^{4}EM-2	1:1
4	[Phg]^{3}EM-2	1:4
5	[Phg]^{4}EM-2	3:5
6	[DPhg]^{3}EM-2	1:5
7	[DPhg]^{4}EM-2	1:2

[a] Determined by integration of ^{1}H NMR.

sequential CβH and NH observed in position 3 and 4 of these two analogs, suggest that the side chains are so close that aromatic interactions may exist to stabilize the conformations.

2.2. Structural calculation with NOE restraints

Because of conformational flexibility, restrained molecular dynamics was applied to determine conformation in the case of peptides. We incorporated NOE restraints into theoretical conformational analysis and molecular dynamics. To keep the peptide bond preceding proline in the desired configuration (*cis* or *trans*), the onefold torsional potential with the constant −100 and 100 kcal/mol was imposed to force the *cis* or the *trans* configuration, respectively. For each analog, two sets of conformations were generated, depending on the configuration of this peptide bond. During the MD-SA simulations, all conformers fell into high temperature and stationary state, in which the total energies of respective conformers were within the fluctuation of ±5% and no significant variations were observed for the torsion angles. The averaged standard deviations were all <20° for ϕ and ψ torsion angles. This suggests that the respective conformers derived from the DG/MD-SA calculations are little affected by the solvent molecules. We have displayed the *trans* and *cis* conformational ensembles of ten most convergent and least violated structures of analogs 5 and 2 in Figure 4. The obtained conformational ensembles were subsequently subjected to a cluster analysis using the minimum-variance method and

Table 2. ^{1}H chemical shifts (in ppm) of analogs 5 ([Phg]^{4}EM-2) and 2 ([Hfe]^{3}EM-2) in DMSO-d_6 at 298 K

Residue	NH	δH_α	δH_β	δH_γ	δH_δ	δH_ε	δH_ζ(OH)
Tyr^1							
(*cis*)	8.18	3.33	2.78; 2.83		6.90	6.69	9.42
(*trans*)	8.02	4.19	2.79; 2.95		7.12	6.70	9.35
Pro^2							
(*cis*)		3.55	1.66	1.45; 1.53	3.24; 3.28		
(*trans*)		4.40	1.76; 1.99	1.68; 1.76	3.10; 3.60		
Phe^3							
(*cis*)	8.29	4.69	2.84; 3.11			7.32–7.37	
(*trans*)	7.99	4.68	2.89; 3.06			7.32–7.37	
Phg^4							
(*cis*)	8.35	5.38			7.17–7.31		
(*trans*)	8.44	5.37			7.17–7.31		
Ct_{NH_2}							
(*cis*)	7.68						
(*trans*)	7.40						
Tyr^1							
(*cis*)		3.31	2.54; 2.64		6.99	6.65	9.25
(*trans*)		3.72	2.49; 2.85		7.08	6.66	9.25
Pro^2							
(*cis*)		3.97	1.80	1.64; 1.80	3.23; 3.47		
(*trans*)		4.40	1.89; 2.00	1.81; 1.89	3.34; 3.62		
Hfe^3							
(*cis*)	8.33	4.23	1.79; 1.85	2.43; 2.48		7.13–7.17	
(*trans*)	8.14	4.13	1.79	2.53		7.13–7.17	
Phe^4							
(*cis*)	8.00	4.45	2.82; 2.98			7.21–7.23	
(*trans*)	7.83	4.46	2.85; 3.07			7.21–7.23	
Ct_{NH_2}							
(*cis*)	7.37						
(*trans*)	7.45						

the RMSD of backbone was taken as a measure of the distance between conformations and the criterion to separate families.

Although the spatial orientations of the aromatic rings of their respective residues are somewhat different, the backbones of both *trans* and *cis* conformers of analogs 5 and 2 take similar extended conformations as observed in EM-2. Moreover, the present study also showed that the aromatic side chains of these analogs have a certain amount of positional freedom, and would therefore occupy similar spatial orientations despite the difference between *cis* and *trans* isomers. It was noted that the Phe^4 in C-terminus is free to adopt a rigid conformation that is independent of the correct orientation or the stereochemistry of this residue.[27] The influence of modifications of Hfe in Phe^3 as well as Phg in Phe^4 displays similarity in the biological activity and prolongs half-life of degradation observed in our previous bioassay.[31] It suggests that an active ligand with enzymatic stability should be taken into consideration on the basis of not only the similar overall conformation but also conformational difference in the side chain, including the spatial orientation of the respective residues.

2.3. Distances between aromatic rings

It was described that the position of side chain in Tyr^1, Pro^2, and Phe^4 was on the other side of aromatic ring of Trp^3 in *trans*-EM-1, whereas Tyr^1 and Trp^3 were packed against Pro^2 in one side of backbone called a compact sandwich conformation which was observed in *cis*-EM-1.[13] As for EM-2, two types of aromatic amino acids, Tyr^1 and Phe^3, and a spacer Pro^2 are combined in EM-2, which adopts extended structure in both *cis* and *trans* isomers that only two side chains packed in one side.[15] We summarized the relationship of side chains in EM-2 and its analogs given in Table 4. It is shown that the packing of two side chains, including the pyrrolidine ring of Pro^2, is more predominant than the three side chains packed in one side of backbone. It suggests that the aromatic interactions stabilize the conformation instead of hydrogen bonds in analogs of EM-2, which is devoid of hydrogen bonds as indicated by the NMR temperature studies. On the other hand, introducing D-configuration amino acids in EM-2 appears to force the side chain into the opposite direction and transfer the conformations to lose receptor binding activity.[31]

If the distance of an aromatic ring pair between two centroids was less than 5.5 Å, an interaction of aromatic–aromatic was assumed to exist.[12,32] In this case, we summarized average distances of all analogs between the centroids of aromatic rings (Table 5). It was shown that only few distances within 5.5 Å exist in these analogs. The two most close distances between the side chains of position 3 and 4 occurred in it cis-[Phg]^{4}EM-2 and *trans*-[Phg]^{3}EM-2, but those side chains located in opposite side of backbone, as seen in Table 4. Moreover, the interactions consisted in *trans*-[DPhg]^{3}EM-2 with distances between Tyr^1 and DPhg in position 3 or

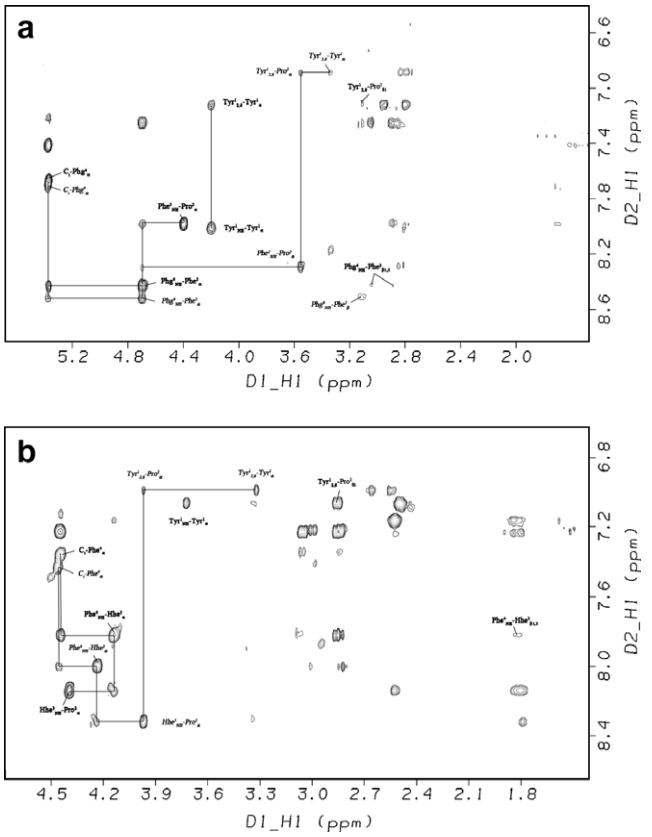

Figure 3. Part of the 500 MHz ROESY spectrums of [Phg]^{4}EM-2 and [Hfe]^{3}EM-2 in DMSO-d_6 at 298 K, showing the assignments of *trans*- (bold) and *cis*- (italic) correlation cross peaks with adjacent amino acids.

4 demonstrate that the conformations of those *trans* analogs may adopt folded structures. The overall distances between centroids of side chain in Tyr^1 and Phe^4 become longer than EM-2 when substituting Hfe/Phg in position 3. Similarly, the distances Tyr^1-Phe^3 also prolong as a substituent is occurring in position 4. It is suggested that the analogs adopt more extended conformations than EM-2 when the distance between aromatic rings and backbone change its pro-active place. We propose that the Cβ in natural phenylalanine may play an important role in maintaining the flexibility and stabilizing the planer of aromatic ring in the interaction with other aromatic side chain.

2.4. Torsions of backbone and side chains

It was demonstrated that in short peptides, when the Xaa-Pro peptide bond exists as a mixture of the *cis* and *trans* isomers, only one isomer was generally proposed to be a bioactive form.[13,33] By measuring the total energies of *cis* and *trans* isomers in EM-2 and its analogs with the lowest energy in ensembles, we found that the all *trans* isomers have somewhat higher energy than the *cis* isomers (Table 6). It is generally known that the energy consumption which transfers the conformation of ligand and receptor to an active status is necessary when a ligand binds to its receptor.[11] Meanwhile, the *trans* isomers of EM-2 analogs were predominant in solution according to the intensities of NH peaks in ^{1}H NMR spectra (Fig. 2). So we proposed the *trans* isomers of analogs to be discussed as mainly bioactive form and the *cis* isomers were artifacts in the solution conditions.[13]

Since the torsion of backbone, ϕ and ψ, can be significantly affected by the slight deviation of side chain,[34] we analyzed the torsion of *trans* isomer for the backbone and side chain in position 3 and 4 (Table 6). Ordering the *trans* isomer with decreasing potency, we found that ϕ_3 of analogs become smaller gradually. Following this tendency, we superpose the $C^2\alpha$ and $C^3\alpha$ of every *trans* analog into those of EM-2 and keep the pair of $C^2\alpha$–$C^3\alpha$–$C^4\alpha$ in same plane. By linking the $C^2\alpha$–$C^3\alpha$–$C^4\alpha$ of EM-2 and its analogs, it is distinct to compare the change of overall backbone trend in position 3 and 4 affected by substitution with different length side chains (Fig. 5). The angles in *trans*-[Phg]^{4}EM-2 and *trans*-[Hfe]^{3}EM-2 have similar or little deviation in contrast with those of EM-2, which cause the side chains in position 3 and 4 to have similar spacial orientation. As for the *trans*-[Hfe]^{4}EM-2 and *trans*-[DPhg]^{4}EM-2, the difference of angle has increased so considerablly that the *trans*-[Phg]^{3}EM-2 and *trans*-[DPhg]^{3}EM-2 show opposite orientations of side chains in Tyr^1 and Phe^4 compared to the extended structure of EM-2. In addition, the different chirality rotated the conformation into folded structure in *trans*-[DPhg]^{3}EM-2. This result revealed that the shortened distance of side chain modified in position 3 involves in great variety with rotating the backbone of N-terminus into another orientation, which leads to the loss of potent in binding to μ-opioid receptor.

The chi (χ) torsional angles of the side chain groups on each amino acid are critical.[30] Although the Phg has no χ^1 angle due to its lack of Cβ, we observed that χ^1 and χ^2 of Hfe in position 3 adopt inverse orientations compared to that in position 4. It is suggested that the restricted configuration of side chain in C-terminus is crucial in stabilizing the conformation to favor the binding of μ-opioid receptor despite its flexibility of preferred structural space.[25]

3. Conclusion

We investigated the conformational requirements of EM-2 analogs containing phenylalanine mimics, phenylglycine (Phg) and homophenylalanine (Hfe), by 1D and 2D ^{1}H NMR spectroscopy and molecular modeling. The different *cis*/*trans* ratios around the Tyr^1-Pro^2 ω bond of analogs were observed in DMSO. The two typical highly potent analogs with similar potent antinociceptive activity as those of EM-2, analogs 5 ([Phg]^{4}EM-2) and 2 ([Hfe]^{3}EM-2), adopted extended conformations obtained by calculation with NOE restraints. Analyses of the relationships of side chains and aromatic interactions by distances of aromatic ring centroids reveal that the proper orientation of the aromatic side chain in position 3 and 4 exhibited different influences on the opioid activity and enzyme stability. Furthermore, the regular variation of dihedral angles

Table 3. Observed NOE cross peaks and intensities of analogs 5 and 2 in DMSO-d_6

NOE cross peaks[a]		NOE intensity[b]	NOE cross peaks		NOE intensity
cis-[Phg]^{4}EM-2			*trans-[Phg]^{4}EM-2*		
$Tyr^1_{NH_2}$	Tyr^1_{α}	Strong	Tyr^1_{α}	$Tyr^1_{2,6H}$	Medium
$Tyr^1_{NH_2}$	$Tyr^1_{\beta1}$	Weak	Tyr^1_{α}	$Pro^2_{\delta1}$	Strong
Tyr^1_{NH2}	$Tyr^1_{\beta2}$	Weak	Tyr^1_{α}	$Pro^2_{\delta2}$	Strong
Tyr^1_{α}	$Tyr^1_{2,6H}$	Strong	$Tyr^1_{2,6H}$	$Pro^2_{\delta1}$	Medium
Tyr^1_{α}	Pro^2_{α}	Strong	Pro^2_{α}	$Pro^2_{\beta1}$	Strong
$Tyr^1_{\beta1}$	$Tyr^1_{2,6H}$	Medium	Pro^2_{α}	$Pro^2_{\beta2}$	Medium
$Tyr^1_{\beta2}$	$Tyr^1_{2,6H}$	Medium	Pro^2_{α}	$Pro^2_{\gamma2}$	Medium
$Tyr^1_{2,6H}$	Pro^2_{α}	Medium	$Pro^2_{\beta1}$	$Pro^2_{\gamma2}$	Strong
Pro^2_{α}	$Pro^2_{\beta1,\beta2}$	Medium	$Pro^2_{\beta1}$	$Pro^2_{\delta2}$	Strong
Pro^2_{α}	$Pro^2_{\gamma1,\gamma2}$	Weak	$Pro^2_{\beta2}$	$Pro^2_{\delta1}$	Medium
$Pro^2_{\beta1,\beta2}$	$Pro^2_{\delta1}$	Strong	$Pro^2_{\gamma1}$	$Pro^2_{\delta2}$	Strong
$Pro^2_{\beta1,\beta2}$	$Pro^2_{\gamma1}$	Medium	Phe^3_{NH}	Phe^3_{α}	Strong
$Pro^2_{\gamma2}$	$Pro^2_{\delta1}$	Strong	Phe^3_{NH}	$Phe^3_{\beta1}$	Strong
$Pro^2_{\gamma1}$	$Pro^2_{\delta2}$	Weak	Phe^3_{α}	$Phe^3_{\beta1}$	Strong
Phe^3_{NH}	Phe^3_{α}	Medium	Phe^3_{α}	$Phe^3_{\beta2}$	Strong
Phe^3_{NH}	$Phe^3_{\beta1}$	Medium	Phg^4_{NH}	Phe^3_{α}	Medium
Phe^3_{NH}	$Phe^3_{\beta2}$	Medium	Phg^4_{NH}	$Phe^3_{\beta1}$	Strong
Phe^3_{α}	Phg^4_{NH}	Medium	Phg^4_{NH}	$Phe^3_{\beta2}$	Medium
Phg^4_{NH}	Phg^4_{α}	Medium	Phg^4_{NH}	Phg^4_{α}	Medium
Phg^4_{α}	Phg^4_{CT}	Strong	Phg^4_{α}	Phg^4_{CT}	Strong
cis-[Hfe]^{3}EM-2			*trans-[Hfe]^{3}EM-2*		
Tyr^1_{α}	$Tyr^1_{2,6H}$	Strong	Tyr^1_{α}	$Tyr^1_{2,6H}$	Medium
Tyr^1_{α}	Pro^2_{α}	Strong	$Tyr^1_{\beta1}$	$Tyr^1_{2,6H}$	Strong
Tyr^1_{α}	Hfe^3_{NH}	Weak	$Tyr^1_{\beta2}$	$Tyr^1_{2,6H}$	Strong
$Tyr^1_{\beta1}$	$Tyr^1_{2,6H}$	Strong	$Tyr^1_{\beta2}$	$Pro^2_{\delta1}$	Medium
$Tyr^1_{\beta2}$	$Tyr^1_{2,6H}$	Strong	$Tyr^1_{2,6H}$	$Pro^2_{\delta1}$	Strong
$Tyr^1_{\beta2}$	Pro^2_{α}	Strong	Pro^2_{α}	$Pro^2_{\beta1}$	Strong
$Tyr^1_{2,6H}$	Pro^2_{α}	Medium	Pro^2_{α}	$Pro^2_{\beta2}$	Strong
Pro^2_{α}	$Pro^2_{\gamma1}$	Medium	Pro^2_{α}	$Pro^2_{\gamma1,\gamma2}$	Medium
Pro^2_{α}	Hfe^3_{NH}	Medium	Pro^2_{α}	Hfe^3_{NH}	Strong
$Pro^2_{\gamma1}$	$Pro^2_{\delta1}$	Strong	$Pro^2_{\beta1}$	$Pro^2_{\gamma1,\gamma2}$	Strong
$Pro^2_{\gamma1}$	$Pro^2_{\delta2}$	Strong	$Pro^2_{\beta1}$	$Pro^2_{\delta2}$	Medium
Hfe^3_{α}	$Hfe^3_{\beta1}$	Medium	$Pro^2_{\gamma1,\gamma2}$	$Pro^2_{\delta2}$	Strong
Hfe^3_{α}	$Hfe^3_{\beta2}$	Strong	Hfe^3_{NH}	Hfe^3_{α}	Strong
Hfe^3_{α}	$Hfe^3_{\gamma1}$	Medium	Hfe^3_{NH}	$Hfe^3_{\beta1,\beta2}$	Strong
Hfe^3_{α}	$Hfe^3_{\gamma2}$	Medium	Hfe^3_{α}	$Hfe^3_{\beta1,\beta2}$	Strong
Hfe^3_{α}	Phe^4_{NH}	Strong	Hfe^3_{α}	$Hfe^3_{\gamma1,\gamma2}$	Medium
$Hfe^3_{\beta1}$	$Hfe^3_{\gamma1}$	Strong	Hfe^3_{α}	Phe^4_{NH}	Strong
$Hfe^3_{\beta1}$	Phg^4_{NH}	Medium	$Hfe^3_{\beta1,\beta2}$	$Hfe^3_{\gamma1,\gamma2}$	Strong
$Hfe^3_{\beta2}$	$Hfe^3_{\gamma2}$	Strong	$Hfe^3_{\beta1,\beta2}$	Phe^4_{NH}	Weak
$Hfe^3_{\beta2}$	Phg^4_{NH}	Strong	Phe^4_{NH}	Phe^4_{α}	Strong
Phe^4_{NH}	Phe^4_{α}	Weak	Phe^4_{NH}	$Phe^4_{\beta1}$	Strong
Phe^4_{NH}	$Phe^4_{\beta1}$	Strong	Phe^4_{NH}	$Phe^4_{\beta2}$	Medium
Phe^4_{NH}	$Phe^4_{\beta2}$	Strong	Phe^4_{α}	Phe^4_{CT}	Strong
Phe^4_{α}	Phe^4_{CT}	Medium			

[a] NOE cross peaks of protons in the same carbon are omitted.
[b] NOE intensities are classified as weak (1.6–5.0 Å), medium (1.6–3.6 Å), and strong (1.6–2.9 Å).

of backbone implied that the spacial conformational properties contain key factors for binding to the μ-opioid receptor. We overlap the angles between Cα in neighbor residues to compare the varying trends from extended to folded following the potency decrease in our previous research. On the basis of these results and discussion, the μ-opioid receptor agonist activity affected by modification of flexibility and chirality of

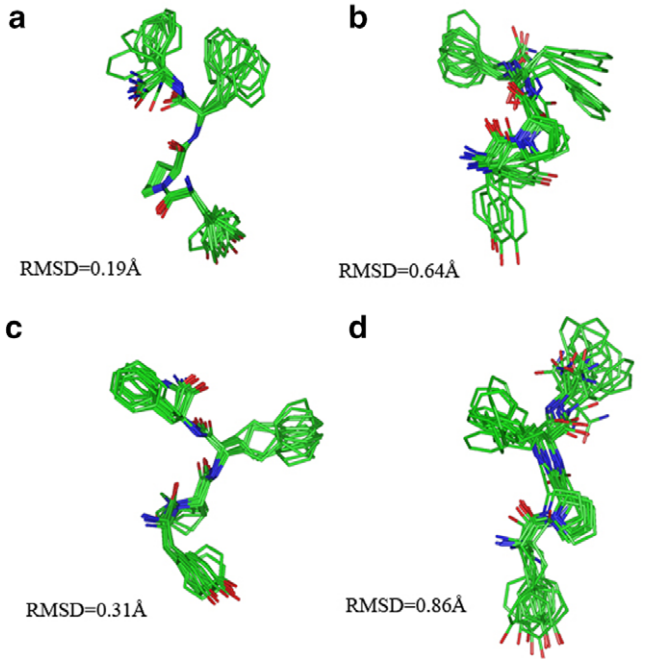

Figure 4. Ensemble of the 10 most convergent and least violated structures of the family (a) *cis*-[Phg]^{4}EM-2, (b) *trans*-[Phg]^{4}EM-2, (c) *cis*-[Hfe]^{3}EM-2, (d) *trans*-[Hfe]^{3}EM-2, as determined by DG calculations and molecular dynamics with NOE distance restraints. The mean backbone RMSD of conformational clusters is labeled.

Table 4. The relationship of aromatic side chains packing in residues of EM-2 and its analogs

Peptides	One side of backbone	Another side of backbone
cis-EM-2	Tyr^1-Phe^3	Pro^2-Phe^4
trans-EM-2	Pro^2-Phe^3	Tyr^1-Phe^4
cis-[Hfe]^{3}EM-2	Pro^2-Phe^4	Tyr^1-Hfe^3
trans-[Hfe]^{3}EM-2	Hfe^3	Tyr^1-Pro^2-Phe^4
cis-[Hfe]^{4}EM-2	Tyr^1-Phe^3	Pro^2-Hfe^4
trans-[Hfe]^{4}EM-2	Phe^3	Tyr^1-Pro^2-Hfe^4
cis-[Phg]^{3}EM-2	Pro^2-Phe^4	Tyr^1-Phg^3
trans-[Phg]^{3}EM-2	Tyr^1-Pro^2-Phe^4	Phg^3
cis-[Phg]^{4}EM-2	Pro^2-Phg^4	Tyr^1-Phe^3
trans-[Phg]^{4}EM-2	Phe^3	Tyr^1-Pro^2-Phg^4
cis-[DPhg]^{3}EM-2	—	—
trans-[DPhg]^{3}EM-2	Tyr^1-Pro^2-Phe^4	DPhg^3
cis-[DPhg]^{4}EM-2	Pro^2-DPhg^4	Tyr^1-Phe^3
trans-[DPhg]^{4}EM-2	Tyr^1-Pro^2-DPhg^4	Phe^3

aromatic side chain requires the peptide structure to retain the proper three-dimensional array of pharmacophores, which is necessary for the development of new native peptide-based analgesics.

4. Experimental

4.1. Peptides

EM-2 and its analogs in this study were synthesized by solution methodology using Boc-amino protection groups and *N*-methyl morpholine (NMM) and isobutyl chloroformate (IBCF) as coupling reagents reported previously, and TFA and anisole (v/v = 9:1) were used as deprotection reagents.[31,35] Mass spectra were measured with MARINER 5074 ESI-TOF analyses (Applied Biosystems, USA). The crude peptides were obtained as TFA salts and then purified using RP-HPLC with Waters Delta-Pak C18 column (3.9 × 150 mm). Purity greater than 99% was verified for all analogs.

Table 5. Average distance (Å) between the centroids of aromatic rings in EM-2 and its analog clusters of 100 conformations

Peptides	R^1–R^{3a}	R^1–R^{4b}	R^3–R^{4c}
cis-EM-2	7.11(11)[d]	9.52(8)	7.82(0)
trans-EM-2	8.54(7)	9.44(4)	7.69(2)
cis-[Hfe]^{3}EM-2	10.56(0)	12.37(0)	10.90(0)
trans-[Hfe]^{3}EM-2	11.04(0)	14.35(0)	8.88(0)
cis-[Hfe]^{4}EM-2	9.13(0)	12.05(0)	9.53(1)
trans-[Hfe]^{4}EM-2	10.81(0)	12.35(0)	8.88(3)
cis-[Phg]^{3}EM-2	7.42(9)	9.88(0)	7.77(1)
trans-[Phg]^{3}EM-2	8.11(11)	10.47(0)	6.07(40)
cis-[Phg]^{4}EM-2	10.23(0)	11.44(0)	5.75(52)
trans-[Phg]^{4}EM-2	8.05(16)	9.01(2)	8.16(3)
cis-[DPhg]^{3}EM-2	—	—	—
trans-[DPhg]^{3}EM-2	8.78(0)	8.75(37)	7.41(1)
cis-[DPhg]^{4}EM-2	9.38(3)	11.35(0)	6.92(14)
trans-[DPhg]^{4}EM-2	9.66(0)	10.07(0)	6.70(27)

[a] Tyr^1 to Phe^3, Hfe^3 or Phg(DPhg)^3.
[b] Tyr^1 to Phe^4, Hfe^4 or Phg(DPhg)^4.
[c] Phe^3, Hfe^3 or Phg(DPhg)^3 and Phe^4, Hfe^4 or Phg(DPhg)^4.
[d] The percentage of distance within 5.5 Å is given in bracket.

4.2. NMR experiments

Peptide samples were dissolved in dimethylsulfoxide-d_6 (DMSO-d_6) (99.9% isotopic purity; Cambridge Isotope Laboratories, Andover, MA) at a concentration of 5–10 mg/500 μL. One-dimensional spectra, which were used to measure the temperature coefficients of the chemical shifts for the amide proton resonances, were recorded in the temperature range 298–318 K. All 2D experiments were performed at 500 MHz on a Varian INOVA NMR spectrometer with a constant temperature at 298 K. The Homonuclear correlation spectra, COSY, TOCSY, and ROESY, were obtained using standard pulse programs. The mixing times of 80 and 300 ms were used for TOCSY and ROESY spectra, respectively.

The 2D NMR matrixes were created and analyzed using the FELIX 2004 computer program (Biosym Technologies Inc., San Diego, CA). Each two-dimensional spectrum was acquired as 1024 × 1024 data matrix complex points in $t1$ and $t2$. The assignments of chemical shifts were carried out using standard protein database and custom unusual amino acid database built artificially. NOE restraints determined from ROESY spectra using correlation between signal strength and interatomic distance were applied in restraint structural calculation by the criteria of 1.70 Å between two Cβ protons.

4.3. Computational molecular modeling

All the molecular modeling calculations were performed on an Origin 2000 workstation running the Irix 6.5

Table 6. Energy (kcal) of *cis* and *trans* isomers, and dihedral angles (°) of backbone (ϕ, ψ) and side chain (χ^1, χ^2) for the *trans* isomer in analogs of EM-2 with the lowest energy calculated conformation sorted order as bioactivity decreases

Peptides	*cis*	*trans*	ψ_1	χ_1^1	ϕ_2	ψ_2	χ_2^1	ϕ_3	ψ_3	χ_3^1	χ_3^2	ϕ_4	ψ_4	χ_4^1	χ_4^2
EM-2	150.3	238.9	60.2	30.8	−57.1	−13.7	22.0	−155.1	−177.3	27.5	—	−90.6	155.7	18.6	—
[Phg]^{4}EM-2	162.0	224.8	131.6	−178.4	−29.8	−84.3	−47.6	−120.1	171.9	51.4	—	−120.0	114.3	—	—
[Hfe]^{3}EM-2	174.9	196.8	−40.2	−20.9	−88.8	148.8	14.1	−84.0	151.7	−29.9	138.1	−91.7	25.4	−159.0	—
[Hfe]^{4}EM-2	196.8	278.1	−77.0	25.2	−68.4	129.2	26.4	−60.8	147.5	−124.4		75.1	117.5	−134.1	−96.5
[DPhg]^{4}EM-2	176.0	240.6	159.2	56.4	−84.5	135.6	29.5	−53.4	136.8	86.4	—	24.7	−119.4	—	—
[Phg]^{3}EM-2	175.9	211.4	157.0	57.8	−44.7	88.7	−15.0	−44.9	−98.8	—	—	−91.2	162.3	23.3	—
[DPhg]^{3}EM-2	—	226.7	123.4	15.7	−78.9	−2.0	48.5	−42.4	−73.7	—	—	−11.5	116.2	−161.3	—

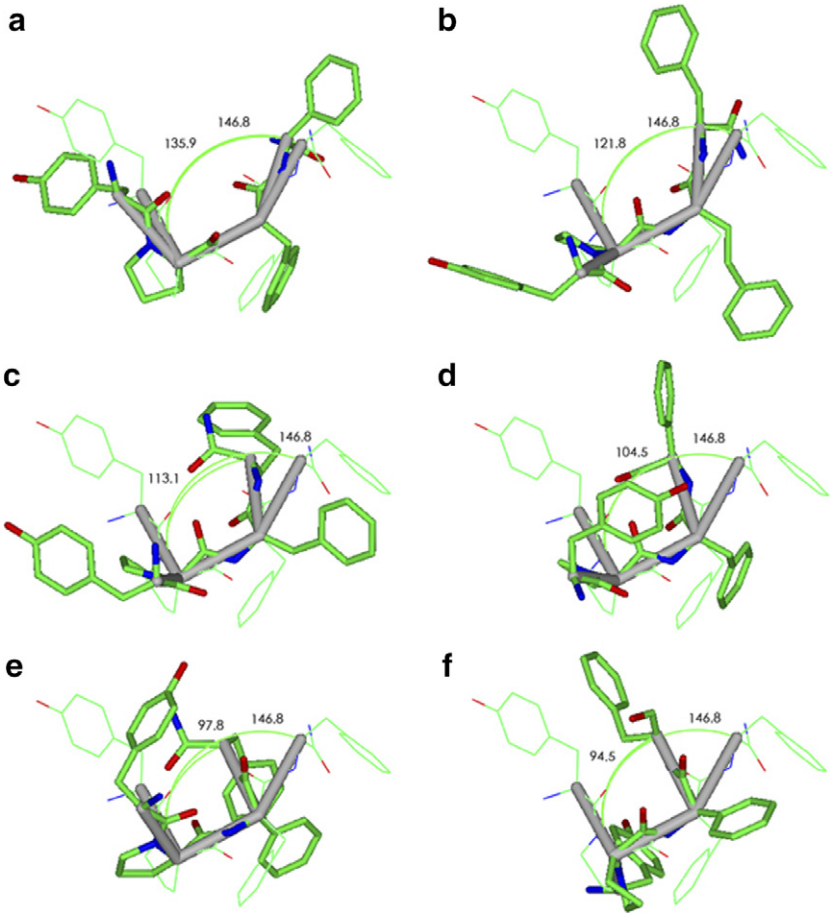

Figure 5. Comparison of the plane angles $C^2\alpha$–$C^3\alpha$–$C^4\alpha$ in EM-2 (shown in line) and its analogs (shown in stick) sorted by bioactivity decreases. (a) *trans*-[Phg]^{4}EM-2, (b) *trans*-[Hfe]^{3}EM-2, (c) *trans*-[Hfe]^{4}EM-2, (d) *trans*-[DPhg]^{4}EM-2, (e) *trans*-[Phg]^{3}EM-2, (f) *trans*-[DPhg]^{3}EM-2. The backbone trends have been shown in thick stick and the degrees of angles in EM-2 and its analogs have been labeled, respectively.

operation system (Silicon Graphics Inc., Mountain View, CA, USA). The initial random molecular structures were built for two isomers with ω torsion angles of Tyr^1-Pro^2 bond in allowance of 0° ± 10° and 180° ± 10°, respectively. And then energy minimizations in vacuo with the CVFF force field (Accelrys Inc.) were carried out on Discover 98 module in the Insight II 2000 package (Accelrys Inc.). The resulting coordinates were applied in the generation of the distance-bound matrixes. Calculating by the standard protocol of the Distance Geometry (DG) II package in NMR-Refine module of Insight II 2000 with NOE restraints files exported from Felix2004. First, triangle bound smoothing was used to check out the correction of molecular structure by minimization. The force constant used for distance restraints was 50.0 kcal/mol Å^2. Second, the structures were used to generate in four dimensions, then reduced to three dimensions with the EMBED algorithm.[36] Third, the assembly was optimized with a simulated annealing (SA) step[37] maintaining the distance constraints according to the standard protocol of the DG II package. Hundred structural ensembles were generated for every system.

In order to investigate the effect of solvents on the peptide conformations, the representative conformers generated by the above calculations were further subjected to molecular dynamics-simulated annealing (MD-SA) using the Discover program. The simulation was performed on the molecule in a 30 Å TIP3 water-

box with the CVFF force field. The energy of the system was minimized and SA simulation was then performed, heating stepwise to a final temperature of 600 K. Gradual temperature reduction to 300 K, 20 ps equilibration, and a 10 ps production period followed. Restrained MD simulations covering 100 ps were then carried out, in which the energy term for distance restraint was treated in the same way as the SA calculation. For each DG structure, MD simulation consisted of 10 ps at 300 K, time step 1.0 fs, temperature relaxation time 0.02 ps, and a period of update of nonbonded atom list 25 fs. On the basis of the root mean square deviation (RMSD) of backbone, each ensemble of the 10 most convergent and least violated conformations of EM-2 and its analogs was selected. Energies and pharmacophoric distances were measured from these DG/MD-SA structures.

Acknowledgments

This work was supported by the grants from the National Natural Science Foundation of China (Nos. 20525206, 20472026), and by Chang Jiang Scholar Program and the Specialized Research Fund for the Doctoral Program in Higher Education Institutions of the Ministry of Education of China.

References and notes

1. Burley, S. K.; Petsko, G. A. *Science* **1985**, *229*, 23.
2. Burley, S. K.; Petsko, G. A. *FEBS Lett.* **1986**, *203*, 139.
3. Blundell, T.; Singh, J.; Thornton, J.; Burley, S. K. *Science* **1986**, *234*, 1005.
4. Waters, M. L. *Curr. Opin. Chem. Biol.* **2002**, *6*, 736.
5. Waters, M. L. *Biopolymers* **2004**, *76*, 435.
6. Chelli, R.; Gervasio, F. L.; Procacci, P.; Schettino, V. *J. Am. Chem. Soc.* **2002**, *124*, 6133.
7. Serrano, L.; Bycroft, M.; Fersht, A. R. *J. Mol. Biol.* **1991**, *218*, 465.
8. Sapse, A. M.; Schweitzer, B. S.; Dicker, A. P.; Bertino, J. R.; Frecer, V. *Int. J. Pept. Protein Res.* **1992**, *39*, 18.
9. Ren, T.; Jin, Y.; Kim, K. S.; Kim, D. H. *J. Biomol. Struct. Dyn.* **1997**, *15*, 401.
10. Zadina, J. E.; Hackler, L.; Ge, L. J.; Kastin, A. J. *Nature* **1997**, *386*, 499.
11. Gentilucci, L.; Tolomelli, A. *Curr. Top. Med. Chem.* **2004**, *4*, 105.
12. Leitgeb, B.; Tóth, G. *Eur. J. Med. Chem.* **2005**, *40*, 674.
13. Podlogar, B. L.; Paterlini, M. G.; Ferguson, D. M.; Leo, G. C.; Demeter, D. A.; Brown, F. K.; Reitz, A. B. *FEBS Lett.* **1998**, *439*, 13.
14. Fiori, S.; Renner, C.; Cramer, J.; Pegoraro, S.; Moroder, L. *J. Mol. Biol.* **1999**, *291*, 163.
15. In, Y.; Minoura, K.; Ohishi, H.; Minakata, H.; Kamigauchi, M.; Sugiura, M.; Ishida, T. *J. Pept. Res.* **2001**, *58*, 399.
16. In, Y.; Minoura, K.; Tomoo, K.; Sasaki, Y.; Lazarus, L. H.; Okada, Y.; Ishida, T. *FEBS J.* **2005**, *272*, 5079.
17. Okada, Y.; Fukumizu, A.; Takahashi, M.; Shimizu, Y.; Tsuda, Y.; Yokoi, T.; Bryant, S. D.; Lazarus, L. H. *Biochem. Biophys. Res. Commun.* **2000**, *276*, 7.
18. Leitgeb, B.; Szekeres, A.; Tóth, G. *J. Pept. Res.* **2003**, *62*, 145.
19. Leitgeb, B.; Ötvös, F.; Tóth, G. *Biopolymers* **2003**, *68*, 497.
20. Leitgeb, B.; Szekeres, A. *J. Mol. Struct. Theochem* **2003**, *666*, 337.
21. Ötvös, F.; Kortvelyesi, T.; Tóth, G. *J. Mol. Struct. Theochem* **2003**, *666*, 345.
22. Cardillo, G.; Gentilucci, L.; Melchiorre, P.; Spampinato, S. *Bioorg. Med. Chem. Lett.* **2000**, *10*, 2755.
23. Cardillo, G.; Gentilucci, L.; Qasem, A. R.; Sgarzi, F.; Spampinato, S. *J. Med. Chem.* **2002**, *45*, 2571.
24. Cardillo, G.; Gentilucci, L.; Tolomelli, A.; Calienni, M.; Qasem, A. R.; Spampinato, S. *Org. Biomol. Chem.* **2003**, *1*, 1498.
25. Tömböly, C.; Köver, K. E.; Péter, A.; Tourwé, D.; Biyashev, D.; Benyhe, S.; Borsodi, A.; Al-Khrasani, M.; Rónai, A. Z.; Tóth, G. *J. Med. Chem.* **2004**, *47*, 735.
26. Eguchi, M.; Shen, R. Y. W.; Shea, J. P.; Lee, M. S.; Kahn, M. *J. Med. Chem.* **2002**, *45*, 1395.
27. Paterlini, M. G.; Avitabile, F.; Ostrowski, B. G.; Ferguson, D. M.; Portoghese, P. S. *Biophys. J.* **2000**, *78*, 590.
28. Keller, M.; Boissard, C.; Patiny, L.; Chung, N. N.; Lemieux, C.; Mutter, M.; Schiller, P. W. *J. Med. Chem.* **2001**, *44*, 3896.
29. Schwyzer, R. *Ann. N Y Acad. Sci.* **1977**, *297*, 3.
30. Cowell, S. M.; Lee, Y. S.; Cain, J. P.; Hruby, V. *J. Curr. Med. Chem.* **2004**, *11*, 2785.
31. Gao, Y.; Liu, X.; Liu, W.; Qi, Y.; Liu, X.; Zhou, Y.; Wang, R. *Bioorg. Med. Chem. Lett.* **2006**, *16*, 3688.
32. Brandl, M.; Weiss, M. S.; Jabs, A.; Suhnel, J.; Hilgenfeld, R. *J. Mol. Biol.* **2001**, *307*, 357.
33. Grathwohl, C.; Wüthrich, K. *Biopolymers* **1981**, *20*, 2623.
34. Chakrabarti, P.; Pal, D. *Protein Eng.* **1998**, *11*, 631.
35. Wei, J.; Shao, X.; Gong, M. Z.; Zhu, B. B.; Cui, Y. X.; Gao, Y. F.; Wang, R. *Bioorg. Med. Chem. Lett.* **2005**, *15*, 2986.
36. Crippen, G. M., Havel, T.F. 1988. *Distance Geometry and Molecular Conformation*. Research Studies Press: Somerset, England and John Wiley: New York, 1988.
37. Nilges, M.; Clore, G. M.; Gronenborn, A. M. *FEBS Lett.* **1988**, *239*, 129.